Inorg. Chem. **2003**, *42*, 3374–3382

Iron-Promoted Nucleophilic Additions to Diimine-Type Ligands: A Synthetic and Structural Study

Ana Tesouro Vallina,[†] Helen Stoeckli-Evans,[‡] Antonia Neels,[‡] JUrgen Ensling,[§] and Silvio Decurtins*[,†]

Departement für Chemie und Biochemie, Universität Bern, Freiestrasse 3, CH-3012 Bern, Switzerland, Institut de Chimie, Université de Neuchâtel, Avenue Bellevaux 51, CH-2007 Neuchâtel, Switzerland, and Institut für Anorganische Chemie und Analytische Chemie Johannes Gutenberg-Universität, Staudingerweg 9, D-55099 Mainz, Germany

Received October 2, 2002

We report here three examples of the reactivity of protic nucleophiles with diimine-type ligands in the presence of Fe^{II} salts. In the first case, the iron-promoted alcoholysis reaction of one nitrile group of the ligand 2,3-dicyano-5,6-bis(2-pyridyl)-pyrazine (L1) permitted the isolation of an stable *E*-imido–ester, $[Fe(L1')_2](CF_3SO_3)_2$ (**1**), which has been characterized by spectroscopic studies (IR, ES-MS, Mössbauer), elemental analysis, and crystallographically. Compound **1** consists of mononuclear octahedrally coordinated Fe^{II} complexes where the Fe^{II} ion is in its low-spin state. The iron-mediated nucleophilic attack of water to the asymmetric ligand 2,3-bis(2-pyridyl)pyrido[3,4-*b*]pyrazine (L2) has also been studied. In this context, the crystal structures of two hydration–oxidation Fe^{III} products, $[Fe(L2')_2](ClO_4)_3 \cdot 3CH_3CN$ (**2**) and *trans*-$[FeL2''Cl_2]$ (**3**), are described. Compounds **2** and **3** are both mononuclear Fe^{III} complexes where the metals occupy octahedral positions. In principle, L2 is expected to coordinate to metal ions through its bipyridine-type units to form a five-membered ring; however, this is not the case in compounds **2** and **3**. In **2**, the ligand coordinates through its pyridines and through the hydroxyl group attached to the pyrazine imino carbon after hydration, that is, in an N,O,N tridentate manner. In compound **3**, the ligand has suffered further transformations leading to a very stable diamido complex. In this case, the metal ion achieves its octahedral geometry by means of two pyridines, two amido N atoms, and two axial chlorine atoms. Magnetic susceptibility measurements confirmed the spin state of these two Fe^{III} species: compounds **2** and **3** are low-spin and high-spin, respectively.

Introduction

Diimine-type ligands are widely used in coordination chemistry due to their good properties as chelating agents, their stability, and their facility to form complexes with a large variety of metal ions. We are currently investigating the synthesis of new iron complexes with diimine-type ligands. In this context, we have synthesized and characterized the ligands 2,3-dicyano-5,6-bis(2-pyridyl)-pyrazine (L1) and 2,3-bis(2-pyridyl)pyrido[3,4-*b*]pyrazine (L2) and have studied their reactivity with iron salts under different conditions. Compared with the ligand bis-2,3-(2-pyridyl)-pyrazine (bpp), L1 contains two additional nitrile functions whereas L2 includes an asymmetrical unit, the pyrido ring attached to the pyrazine.

The reactions involving addition of alcohols, amines, water, or other nucleophiles to nitriles very often require high temperatures, long reaction times, and the use of either basic or acid conditions.[1,2] In many cases, the reaction conditions can be softened by using metal ions.[3] In fact, the coordination of the metal ion to the nitrile N atom or to other donor groups of the ligand increases the electrophilic nature of the nitrile carbon making it more predisposed to nucleophilic attack. Sometimes, the nitrile groups are stable in the presence of

* To whom correspondence should be addressed. E-mail: silvio.decurtins@iac.unibe.ch.
[†] Universität Bern.
[‡] Université de Neuchâtel.
[§] Institut für Anorganische Chemie und Analytische Chemie Johannes Gutenberg-Universität.

(1) (a) Vollhardt, K. P. C.; Schore, N. E. *Organic Chemistry: Structure and function*; W. H. Freeman: New York, 1999. (b) Alves, M. J.; Carvalho, M. A.; Proenca, M. F. J. R. P.; Booth, B. L. *J. Heterocycl. Chem.* **2000**, *37*, 1041. (c) Jones, M. M. *Ligand Reactivity and Catalysis*; Academic Press: New York, 1968. (d) Constable, E. C. *Metals and Ligand Reactivity, an Introduction to the Organic Chemistry of Metal Complexes*; VCH: Weinheim, 1996.
(2) Robinson, B. *J. Chem. Soc.* **1963**, 2417.

10.1021/ic026079l CCC: $25.00
Published on Web 04/23/2003

alcohols, water, or metals.[4] The reactions of nitriles, R−C≡N, as part of transition metal complexes that cause the formation of new organic ligands as a result of different chemical processes, like insertion, coupling, reduction, and nucleophilic or electrophilic attack, have been thoroughly studied, and they have important implications in chemistry.[5,6] The resulting molecule is stabilized by complex formation, and in some cases, intermediates, which are otherwise of difficult to obtain, can be isolated. These reactions include metal ions such as Pt, Pd, Rh, W, Ru, Cu, Ni, or Co.[7−10] Although a considerable number of imido−ester complexes have been described in the literature, their crystal structures have been scarcely reported.[11−17]

The ligand 2,3-bis(2-pyridyl)pyrido[3,4-*b*]pyrazine, L2, belongs to the family of the pyrido[3,4-*b*]pyrazines. These heterocycles are normally stable in the neutral form but are rapidly hydrated if the pyridine nitrogen atom is protonated. The degree of hydration depends on the pyrazine ring substituents.[18] Gordon et al.[19] have described the synthesis as well as spectroscopic and electrochemical studies of a series of bimetallic rhenium(I) complexes with different asymmetric polypyridyl ligands, including some with the ligand L2. These are, to our knowledge, the only metal complexes reported with this ligand.

We report here the crystal structures of three new mononuclear Fe^{II} and Fe^{III} complexes obtained from reactions with the ligands L1 and L2. Compound **1**, $[Fe(L1')_2](CF_3SO_3)_2$, is, to our knowledge, the first example of an imido−ester stabilized by Fe^{II} and characterized by single-crystal X-ray diffraction. Compound **2**, $[Fe(L2')_2](ClO_4)_3 \cdot 3CH_3CN$, is a unique example of an iron-mediated addition of water to a pyrido[3,4-*b*]pyrazine. In contrast with the nucleophilic additions to nitriles, the addition of water to diimines has not been often observed. Bandoli et al.[20] have described what is, to our knowledge, the only previous example of a nucleophilic addition of water to a pyrazine-containing ligand, in this case, in the presence of rhenium(V). Finally, we also report the crystal structure of complex **3**, *trans*-$[FeL2''Cl_2]$. In this case, ligand L2 has been initially hydrated, as in compound **2**, and then, it has suffered an additional oxidation to yield a deprotonated diamide mononuclear Fe^{III} complex. Several authors have studied the oxygenation and/or oxidation of a variety of pyrazine derivatives using different conditions, for instance, by photooxygenation[21,22] or by heating in acid conditions[23] or in the presence of H_2O_2 in acetic acid[24] to occasionally obtain the corresponding amide compounds. In addition, it is worth noting that, before the oxidation step, a reduction of the pyrazine to the hydropyrazine is sometimes required.

Experimental Section

(A) Materials and Methods. All chemicals were used as received without further purification. All solvents were purchased from Fluka (puris., 99.8%, H_2O < 0.01%, over molecular sieves) and stored under nitrogen. Caution! Perchlorate salts with organic ligands are potentially explosive and should be handled with the necessary precautions. ^1H and ^{13}C NMR spectra were recorded on a Bruker AC-300 spectrometer and calibrated against the deuterated solvent. Chemical shifts (δ) are given in ppm, and coupling constants (J) are given in hertz. Infrared spectra were obtained with a Perkin-Elmer Spectrum One FT-IR spectrometer using KBr pellets. Electrospray (ESI) mass spectra were performed using a Sciex Q-Star system. Magnetic susceptibility data of the powdered polycrystalline samples were collected with an MPMS Quantum Design SQUID magnetometer in the temperature range 300−1.8 K at a field of 1000 G. The output data were corrected for the diamagnetism of the sample holder and the diamagnetism of the samples calculated from Pascal's constants. Mössbauer spectroscopy measurements were performed on a constant-acceleration type Mössbauer spectrometer together with a 1024-channel analyzer

(3) (a) Baker, W. A.; Daniels, M. *J. Inorg. Nucl. Chem.* **1963**, 1194. (b) Sánchez, G.; Serrano, J. L.; Ramírez de Arellano, M. C.; Pérez, J.; López, G. *Polyhedron* **2000**, *19*, 1395. (c) Hvastijova, M.; Kohout, J.; Kozisek, J.; Svoboda, I. *J. Coord. Chem.* **1999**, *47*, 573. (d) Bakir, M.; McKenzie, J. A. M. *J. Chem. Soc., Dalton Trans.* **1997**, *19*, 3571. (e) Lakouraj, M. M.; Movassagh, B.; Fasihi, J. *Synth. Commun.* **2000**, *30*, 821. (f) Murahashi, S.-I.; Takaya, H. *Acc. Chem. Res.* **2000**, *33*, 225.

(4) (a) Simão, D.; Alves, H.; Belo, D.; Rabaça, S.; Branco Lopes, E.; Cordeiro Santos, I.; Gama, V.; Duarte, M. T.; Teives Henriques, R.; Novais, H.; Almeida, M. *Eur. J. Inorg. Chem.* **2001**, 3119. (b) Batsanov, A. S.; Begley, M. J.; George, M. W.; Hubberstey, P.; Munakata, M.; Russell, C. E.; Walton, P. H. *J. Chem. Soc., Dalton Trans.* **1999**, 4251. (c) Rossenbeck, B.; Sheldrick, W. S. *Z. Naturforsch., B: Chem. Sci.* **1999**, *54*, 1510. (d) Mayr, A.; Mao, L.-F. *Inorg. Chem.* **1998**, *37*, 5776. (e) Jacob, V.; Mann, S.; Huttner, G.; Walter, O.; Zsolnai, L.; Kaifer, E.; Rutsch, P.; Kircher, P.; Bill, E. *Eur. J. Inorg. Chem.* **2001**, 2625. (f) Hirano, M.; Kiyota, S.; Imoto, M.; Komiya, S. *Chem. Commun.* **2000**, 1679. (g) Chin, J.; Kim, J. H. *Angew. Chem., Int. Ed. Engl.* **1990**, *29*, 523.

(5) Storhoff, B. N.; Lewis, H. C. *Coord. Chem. Rev.* **1977**, *23*, 1.

(6) Michelin, R.; Mozzon, M.; Bertani, R. *Coord. Chem. Rev.* **1996**, *147*, 299.

(7) Wada, M.; Shimohigashi, T. *Inorg. Chem.* **1976**, *15*, 954.

(8) (a) Suzuki, S.; Nakahara, M.; Watanabe, K. *Bull. Chem. Soc. Jpn.* **1971**, *44*, 1441. (b) Clark, C. R.; Hay, R. W. *J. Chem. Soc., Dalton Trans.* **1974**, 2148. (c) Breslow, R.; Schmir, M. *J. Am. Chem. Soc.* **1971**, *93* (19), 4960.

(9) (a) Paul, P.; Nag, K. *Inorg. Chem.* **1987**, *26*, 1586. (b) Paul, P.; Nag, K. *J. Chem. Soc., Dalton Trans.* **1988**, 2373.

(10) Ros, R.; Renaud, J.; Roulet, R. *J. Organomet. Chem.* **1976**, *104*, 271.

(11) Cini, R.; Caputo, P. A.; Intini, F. P.; Natile, G. *Inorg. Chem.* **1995**, *34*, 1130.

(12) Bokach, N. A.; Kukushkin, V. Y.; Kuznetsov, M. L.; Garnovskii, D. A.; Natile, G.; Pombeiro, A. J. L. *Inorg. Chem.* **2002**, *41*, 2041.

(13) Potts, R. A.; Gaj, D. L.; Schneider, W. F.; Dean, N. S.; Kampf, J. W.; Olivier, J. P. *Polyhedron* **1991**, *10*, 1631.

(14) Masood, Md. A.; Sullivan, B. P.; Hodgson, D. J. *Inorg. Chem.* **1999**, *38*, 5425.

(15) Byers, P.; Drew, M. G. B.; Hudson, M. J.; Isaacs, N. S.; Upadhaya, A.; Madic, C. *Polyhedron* **1994**, *13*, 345.

(16) Jamnický, M.; Segl'a, P.; Koman, M. *Polyhedron* **1995**, *14*, 1837.

(17) Bu, X.-H.; Du, M.; Tanaka, K.; Shionoya, M.; Shiro, M. *Inorg. Chem. Commun.* **2001**, *4*, 150.

(18) (a) Cheeseman, G. W. H.; Cookson, R. F. *The Chemistry of Heterocyclic compounds: Condensed pyrazines*; John Wiley & Sons: New York, 1979; Vol. 35, Chapters 28 and 29. (b) Cushman, M.; Wong, W. C.; Bacher, A. *J. Chem. Soc., Perkin Trans. 1* **1986**, *6*, 1043.

(19) (a) Simpson, T. J.; Gordon, K. C. *Inorg. Chem.* **1995**, *34*, 6323. (b) Abbott, L. C.; Arnold, C. J.; Gordon, K. C.; Hester, R. E.; Moore, J. N.; Perutz, R. N.; Ye, T.-Q. *Laser Chem.* **1999**, *19*, 279.

(20) Bandoli, G.; Gerber, T. I. A.; Jacobs, R.; du Preez, J. G. H. *Inorg. Chem.* **1994**, *33*, 178.

(21) (a) Markham, J. L.; Sammes, P. G. *J. Chem. Soc., Perkin Trans. 1* **1979**, *7*, 1885. (b) Nishio, T.; Kondo, M.; Omote, Y. *J. Chem. Soc., Perkin Trans. 1* **1985**, *11*, 2497.

(22) (a) Adam, W.; Ahrweiler, M.; Vlcek, P. *J. Am. Chem. Soc.* **1995**, *117*, 9690. (b) Brook, D. J. R.; Haltiwanger, R. C.; Koch, T. H. *J. Am. Chem. Soc.* **1992**, *114*, 6017.

(23) Lunsford, C. D.; Lutz, R. E.; Bowden, E. E. *J. Org. Chem.* **1955**, *20*, 1513.

(24) Barton, J. W.; Goodland, M. C.; Gould, K. J.; Hadley, J.; McOmie, J. F. W. *Polyhedron* **1978**, *34*, 495.

operating in the time scale mode. The source, ^{57}Co/Rh (25 mCi, Amersham Buchler), was kept at room temperature for all measurements. The velocity calibration was performed with the known hyperfine splittings in the spectrum of metallic iron, and the isomer shifts reported here are collected between 293 and 135 K by means of a He continuous flow cryostat (model CF500, Oxford Instruments).

2,3-Dicyano-5,6-bis(2-pyridyl)-pyrazine (L1) was prepared by Schiff base condensation of equimolar amounts of 2,2′-pyridyl (2,12 g, 10 mmol) and diaminomaleonitrile (1.08 g, 10 mmol) in ethanol (40 mL) at reflux for ca. 3 h. After the reaction was stopped, the mixture was immediately filtered to remove the brown impurities. Then, the solution was passed over active carbon, and the solvent was removed under vacuum. Recrystallization from ethanol yielded L1 as pale yellow crystals (0.85 g, 30% yield). Anal. for $C_{16}H_8N_6$ Found: C, 67.50; H, 2.75; N, 29.80. Calcd: C, 67.60; H, 2.84; N, 29.56. FAB$^+$-MS: 285 (M^+, 100). IR (KBr pellet, cm^{-1}): 3436 (br, w), 3068 (w), 2403 (w), 2308 (w), 2242 (w), 1994 (w), 1969 (w), 1588 (s), 1571 (m), 1523 (m), 1473 (m), 1438 (m), 1386 (vs), 1299 (w), 1283 (m), 1247 (m), 1234 (m), 1200 (m), 1153 (m), 1131 (m), 1097 (s), 1049 (m), 996 (s), 975 (w), 960 (w), 895 (w), 824 (m), 793 (s), 741 (s), 711 (w). ^{1}H NMR ($CDCl_3$): 7.33 (2H, m), 7.90 (2H, m), 8.06 (2H, d, $J = 8$ Hz), 8.31 (2H, d, $J = 4.0$ Hz) ppm. ^{13}C NMR ($CDCl_3$): 113.0, 124.7, 124.8, 130.2, 137.2, 148.9, 153.9, 154.9 ppm.

2,3-Bis(2-pyridyl)pyrido[3,4-*b*]pyrazine (L2) was prepared following a similar procedure by condensation of equimolar amounts of 2,2′-pyridyl and 3,4-diaminopyridine in ethanol at reflux over ca. 3 h. Removal of solvent afforded a powder that was recrystallized in ethanol to give L2 in 50% yield. Anal. for $C_{17}H_{11}N_5$ Found: C, 71.28; H, 3.88; N, 24.68. Calcd: C, 71.57; H, 3.89; N, 24.55. EI$^+$-MS: 285 (M, 100), 285 (M^+, 10). IR (KBr pellet, cm^{-1}): 3048 (m), 2999 (m), 2933 (w), 1588 (s), 1566 (s), 1547 (m), 1471 (s), 1445 (w), 1433 (m), 1423 (m), 1385 (s), 1347 (m), 1330 (m), 1280 (w), 1265 (m), 1242 (m), 1217 (w), 1150 (m), 1095 (w), 1076 (s), 1044 (m), 999 (s), 986 (s), 930 (w), 900 (m), 839 (s), 827 (s), 800 (s), 787 (s), 744 (s), 706 (m). ^{1}H NMR ($CDCl_3$): 7.27 (2H, m), 7.86 (2H, tt), 8.04 (3H, m), 8.35 (2H, m), 8.88 (2H, d), 9.66 (1H, d) ppm. ^{13}C NMR ($CDCl_3$): 156.8, 156.6, 154.5, 148.6, 148.5, 147.8, 143.5, 136.8, 136.7, 136.0, 124.2, 124.1, 123.5, 123.3, 121.41 ppm.

Notation. We have named L1′ the imido−ester form of L1 in complex **1**, L2′ the hydrated form of L2 in complex **2**, and L2″ the bis-amido form of L2 in complex **3**.

[Fe(L1′)$_2$](CF$_3$SO$_3$)$_2$ (1). To an ethanolic (10 mL) solution of L1 (18 mg, 0.06 mmol) was added $FeCl_2 \cdot 4H_2O$ (13 mg, 0.06 mmol) under nitrogen. The color of the solution changed to deep blue after some minutes of heating. The mixture was refluxed for about half an hour, and then $NaCF_3SO_3$ (22 mg, 0.12 mmol) was added. Reflux was continued for another 2 h. Then, the solution was filtered and allowed to evaporate slowly. After a few days, rodlike dark deep blue crystals of **1** were formed. The crystals (60% yield) are air and moisture stable. Anal. for $C_{38}H_{28}F_6FeN_{12}O_8S_2$ Found: C, 44.66; H, 3.07; N, 16.48. Calcd: C, 44.98; H, 2.78; N, 16.56. IR (KBr pellet, cm^{-1}): 3432 (m), 3290 (m), 2999 (w), 2928 (w), 2243 (w), 1693 (w), 1611 (s), 1568 (m), 1542 (m), 1467 (m), 1452 (w), 1428 (m), 1391 (vs), 1352 (m), 1270 (m), 1253 (m), 1235 (m), 1199 (m), 1142 (m), 1028 (w), 1001 (m), 895 (m), 815 (w), 794 (m), 762 (s), 744 (m). ESI-MS *m*/*z*: 865, $[Fe(L1')_2(CF_3SO_3)]^+$, 715 $[Fe(L1')_2 - H^+]^+$, 358, $[Fe(L1')_2]^{2+}$, 330, $[L1'H]^+$.

[Fe(L2′)$_2$](ClO$_4$)$_3$·3CH$_3$CN (2). To a CH_3CN (10 mL) solution of L2 (33 mg, 0.12 mmol) was added $Fe(OH_2)_6 \cdot (ClO_4)_2$ (42 mg, 0.12 mmol) under nitrogen. The color of the solution changed from light yellow to deep brown-orange after a few minutes. The mixture was stirred at RT (room temperature) for about 4 h, filtered, and allowed to evaporate slowly. After one week, brown-orange blocklike crystals (40% yield) of **2** were formed. Anal. for $C_{34}H_{26}Cl_3FeN_{10}O_{14}$ (made on dried powdered crystals) Found: C, 42.22; H, 2.97; N, 14.24. Calcd: C, 42.50; H, 2.73; N, 14.58. IR (KBr pellet, cm^{-1}): 3245 (m), 3090 (m), 2940 (m), 2256 (w), 1646 (s), 1597 (m), 1577 (w), 1560 (m), 1528 (s), 1471 (m), 1440 (m), 1404 (w), 1375 (w), 1356 (w), 1300 (m), 1238 (m), 1159 (s), 1102 (vs), 1044 (s), 932 (m), 818 (m), 798 (m), 781 (m), 769 (m), 706 (m), 624 (s), 578 (m), 567 (m). ESI-MS *m*/*z*: 660, $[Fe(L2')_2 - 2H^+]^+$, 330, $[Fe(L2')_2 - H^+]^{2+}$, 286, $L2H^+$.

***trans*-[FeL2″Cl$_2$] (3).** This compound can be obtained using different procedures: (a) by aerobic slow diffusion of the ligand L2 in CH_2Cl_2 and $FeCl_2 \cdot 4H_2O$ in MeOH; (b) by slow diffusion in a sealed H-tube of CH_3CN solutions of both ligand and metal salt; or (c) by stirring under aerobic conditions equimolar solutions of both reactants in solvents, such as EtOH, CH_3CN, or $MeNO_2$, for ca. 3 h at RT. In the last case, complex **3** starts to precipitate after a few minutes, and stirring is continued in order to complete the reaction. Rodlike dark brown single crystals can be obtained by using slow diffusion techniques, whereas mixing and stirring mainly affords a dark gray microcrystalline powder. It is interesting to note that if the slow diffusion reaction is carried out under argon, crystals start to appear after about 2 months if the tube is not perfectly sealed and air is allowed to enter into the system (20% yield). Anal. for $C_{17}H_{12}Cl_2FeN_5O_2$ Found: C, 45.87; H, 2.64; N, 15.41. Calcd: C, 45.88; H, 2.72; N, 15.74. IR (KBr pellet, cm^{-1}): 3438 (m), 3201 (w), 3139 (w), 3046 (w), 2964 (w), 2923 (w), 2852 (w), 1654 (s), 1633 (m), 1596 (vs), 1570 (w), 1516 (m), 1476 (vs), 1444 (w), 1391 (m), 1340 (vs), 1298 (w), 1283 (w), 1252 (w), 1232 (w), 1157 (m), 1111 (s), 1093 (w), 1049 (m), 1023 (m), 946 (m), 804 (m), 759 (m), 698 (m). ESI-MS (CH_3OH) *m*/*z*: 409, $[FeL2''Cl]^+$, 320, $[H_2L2'']^+$. ESI-MS (H_2O) *m*/*z*: 409, $[FeL2''Cl]^+$, 374, $[FeL2'']^{2+}$.

(B) X-ray Crystal Structure Analysis. The intensity data for all compounds were collected at 153 K on a Stoe image plate diffraction system[25] using Mo Kα graphite monochromated radiation ($\lambda = 0.71073$ Å): image plate distance 70 mm, ϕ oscillation scans 0−190° (for compound **1**) and 0−200° (for compounds **2** and **3**), step $\Delta\phi = 1.0°$ (for **1** and **2**) and 1.1° (for **3**), 2θ range 3.27−52.1°, $d_{max}-d_{min} = 12.45-0.81$ Å. The structures were solved by direct methods using the program SHELXS-97.[26] The refinement and all further calculations were carried out using SHELXL-97.[27] For compound **1**, the NH H-atoms were located from Fourier difference maps and refined isotropically, while the remainder were included in calculated positions and treated as riding atoms using SHELXL-97 default parameters. The non-H atoms were refined anisotropically using weighted full-matrix least-squares on F^2. An empirical absorption correction was applied using the DIFABS routine in PLATON[28] ($T_{min} = 0.116$, $T_{max} = 0.584$). One of the triflate anions is extremely disordered. The best model was initially refined isotropically, except for the S atom which was refined anisotropically and then held fixed in the final cycles of refinement. For compound **2**, the H-atoms were either located from Fourier difference maps and refined isotropically or included in calculated positions and treated as riding atoms using SHELXL-97 default parameters. The non-H atoms were refined anisotropically using

(25) *IPDS Software*; Stoe & Cie GmbH: Darmstadt, Germany, 2000.
(26) Sheldrick, G. M. SHELXS-97 Program for Crystal Structure Determination. *Acta Crystallogr.* **1990**, *A46*, 467.
(27) Sheldrick, G. M. *SHELXL-97*; Universität Göttingen: Göttingen, Germany, 1999.
(28) Spek, A. L. Platon/Pluton v. 1.02.3, 2001. *Acta Crystallogr.* **1990**, *A46*, C-34.

Table 1. Crystallographic Data for Complexes $[Fe(L1')_2](CF_3SO_3)_2$ (**1**), $[Fe(L2')_2](ClO_4)_3 \cdot 3CH_3CN$ (**2**), and $[FeL2''Cl_2]$ (**3**)

	1	**2**	**3**
formula	$C_{38}H_{28}F_6Fe$-$N_{12}O_8S_2$	$C_{40}H_{35}Cl_3Fe$-$N_{13}O_{14}$	$C_{17}H_{12}Cl_2Fe$-N_5O_2
formula mass	1014.69	1084.01	445.07
cryst syst	monoclinic	triclinic	orthorhombic
space group	$P2_1/n$	$P\bar{1}$	$Pbcn$
a (Å)	11.552(1)	12.116(3)	16.879(2)
b (Å)	19.128(1)	12.873(3)	14.071(1)
c (Å)	19.795(2)	15.656(3)	7.223(1)
α (deg)	90	112.13(2)	90.00
β (deg)	96.47(1)	95.04(3)	90.00
γ (deg)	90	96.83(3)	90.00
V (Å^3)	4346.1(5)	2222.4(9)	1715.4(3)
Z	4	2	4
cryst size (mm^3)	0.40 × 0.30 × 0.10	0.40 × 0.25 × 0.18	0.30 × 0.15 × 0.15
D_{calcd} (g·cm^{-3})	1.551	1.620	1.723
μ (mm^{-1})	0.535	0.604	1.215
T_{min}/T_{max}	0.116/0.584		0.433/0.811
reflns indep	8343	8027	1629
reflns obsd	3633, $I > 2\sigma(I)$	4963, $I > 2\sigma(I)$	1248, $I > 2\sigma(I)$
R1[a]	0.0759	0.0519	0.0383
wR2[b]	0.1827	0.1258	0.0893
residual density e/Å^3	1.050/−0.740	1.314/−0.936	0.457/−0.595

[a] $R1(\text{obsd reflns}) = \sum||F_o| - |F_c||/\sum|F_o|$. [b] $wR2(\text{obsd reflns}) = [\sum w(|F_o^2| - |F_c^2|)^2/\sum wF_o^4]^{1/2}$.

weighted full-matrix least-squares on F^2. One of the three perchlorate anions is very disordered with two of the oxygen atoms being split over five positions. Three nondisordered molecules of acetonitrile per unit cell were also located. The methyl-hydrogen atoms of the third acetonitrile molecule were not included due to the high thermal parameter of the carbon atom. Attempts to improve the refinement by splitting C61 and C62 were unsuccessful, and these atoms became nonpositive definite. For compound **3**, the H-atoms were included in calculated positions and treated as riding atoms using SHELXL-97 default parameters. This neutral Fe^{III} complex contains a center of symmetry resulting in partial disorder for atoms C9, N3, and the corresponding riding hydrogen atoms which occupy the same positions with an occupancy of 0.5, respectively. An absorption correction was applied using DIFABS routine in PLATON[28] ($T_{min} = 0.433$, $T_{max} = 0.811$). Crystallographic details for all three compounds are given in Table 1, and significant bond lengths and bond angles are listed in Table 2. Molecular structure and crystallographic numbering schemes are illustrated in the PLATON[28] drawings, Figures 1, 3, and 4. Schemes 1, 3, and 5 show the numbering scheme used to define several significant rings of compounds **1**, **2**, and **3**. A list of the most relevant dihedral angles between some of these rings is also included in Table 2.

Results and Discussion

Complex 1. The crystal structure of **1** is illustrated in Figure 1. The asymmetric unit consists of one dipositive Fe^{II} (LS) complex and two uncoordinated triflate counterions, one of them highly disordered. The coordination site of the Fe^{II} ion may be described as distorted octahedral with four nitrogen atoms, from two pyridine and two pyrazine rings of two ligands L1′, plus two from the imido−esters occupying the vertices of the octahedron. The two imido−ester groups are in a *cis* arrangement with respect to one another. Selected geometrical parameters are given in Table 2. The $Fe-N_{imido}$ and $Fe-N_{py}$ bond distances are comparable to the

Table 2. Selected Bond Distances, Angles, Dihedral Angles, and Short Intra- and Intermolecular Contacts (Å, deg) for Compounds **1**, **2**, and **3**[a]

Distances and Angles for $[Fe(L1')_2](CF_3SO_3)_2$ (**1**)

Fe−N1	1.877(5)	Fe−N7	1.875(5)
Fe−N3	1.960(5)	Fe−N9	1.960(5)
Fe−N5	1.984(5)	Fe−N11	1.951(6)
N5−C15	1.285(8)	N11−C33	1.293(8)
C15−O1	1.323(7)	C33−O2	1.328(8)
C18−N6	1.142(8)	C36−N12	1.160(8)
N7−Fe1−N1	176.2(2)	N11−Fe1−N9	161.5(2)
N3−Fe1−N5	160.9(2)	N3−Fe1−N9	88.7(2)
N7−Fe1−N3	99.4(2)	N11−Fe1−N5	92.1(2)
N11−Fe1−N3	91.7(2)	N7−Fe1−N5	99.7(2)
N1−Fe1−N3	80.7(2)	N7−Fe1−N9	80.6(2)
N1−Fe1−N5	80.3(2)	N7−Fe1−N11	81.1(2)
N5−C15−C4	114.8(5)	N11−C33−C22	114.8(6)

donor-H···acceptor	D−H	H···A	D···A	D−H···A
N11−H11N···O16[i]	0.83(6)	2.17(6)	2.965(8)	158.2(5)
C7−H7a−N12[ii]	0.95	2.49	3.434(8)	175.5

Selected Dihedral Angles between Defined Rings for **1**

1^2	2.21	2^4	89.56	1^6	7.29	8^10	42.75
1^3	84.71	3^4	3.69	1^5	6.19	5^7	50.31
1^4	88.37	3^8	4.39	6^9	69.82		
2^3	86.77	3^9	8.66				

Distances and Angles for $[Fe(L2')_2](ClO_4)_3 \cdot 3CH_3CN$ (**2**)

Fe−O1	1.852(2)	Fe−O2	1.860(2)
Fe−N4	1.963(3)	Fe−N24	1.959(3)
Fe−N5	2.007(3)	Fe−N25	2.008(3)
C1−O1	1.395(4)	C21−O2	1.401(5)
C1−C2	1.528(5)	C21−C22	1.524(5)
C1−N1	1.460(4)	C21−N21	1.453(5)
C2−N2	1.288(5)	C22−N22	1.288(4)
N2−C4	1.404(5)	N22−C23	1.395(5)
O1−Fe1−O2	172.5(1)	O1−Fe1−N24	91.3(1)
N24−Fe1−N5	176.2(1)	O1−Fe1−N4	83.3(1)
N24−Fe1−N25	88.9(1)	N24−Fe1−N4	94.8(1)
Fe1−O1−C1	111.1(2)	Fe1−O2−C21	110.8(2)
O1−C1−N1	110.0(3)	O2−C21−N21	110.5(3)
C2−C1−N1	110.1(3)	C22−C21−N21	110.1(3)

donor-H···acceptor	D−H	H···A	D···A	D−H···A
N1−H1N···O32	0.80(4)	2.18(4)	2.970(5)	169.7(5)
N3−H3N···N61	0.96(6)	1.85(5)	2.772(5)	160.5(5)
N21−H21N···O22[iii]	0.83(5)	2.07(5)	2.885(5)	169.1(5)
N23−H23N···O14[iv]	0.84(5)	2.19(5)	2.878(5)	138.6(5)

Selected Dihedral Angles between Defined Rings for **2**

1^2	73.53	3^4	89.95	8^12	85.35	7^11	87.86
1^3	80.20	1^5	81.17	2^9	78.17	7^8	86.52
1^4	13.02	1^6	82.92	2^10	76.53	11^12	83.53
2^3	8.94	5^6	3.73	9^10	1.89	4^12	3.10
2^4	82.53	3^5	26.16	4^9	26.36	3^8	6.00
2^11	11.53	1^7	4.96				

Distances and Angles for *trans*-$[FeL2''Cl_2]$ (**3**)

Fe1−N1	2.158(2)	O1−C6	1.228(3)
Fe1−N2	2.056(2)	N2−C6	1.365(3)
Fe1−Cl1	2.355(1)	N2−C7	1.385(4)
N2−Fe1−N1	76.7(1)	Cll−Fe1−Cl1[v]	155.4(1)
N2−Fe1−Cl1	97.6(1)	N2−Fe1−N1[v]	153.5(1)
N2[v]−Fe1−N1−C1	−173.5(2)	N1[v]−Fe1−N1−C5	−176.3(2)
Cl1[v]−Fe1−N1−C1	−77.3(2)	Cl1−Fe1−N2−C7	−99.5(2)

donor-H···acceptor	D−H	H···A	D···A	D−H···A
N3−H1N···Cl1[vi]	0.88	2.53	3.346(3)	155.4
C8−H8A···O1 (Intra)	0.95	2.22	2.821(3)	120.0

Selected Dihedral Angles between Defined Rings for **3**

1^2	3.07	2^3	3.07	1^4	1.66
1^3	3.72	2^4	2.01	3^4	4.07

[a] Symmetry operations: i = $^3/_2 - x$, $^1/_2 + y$, $^1/_2 - z$; ii = $-1 + x$, y, z; iii = $1 - x$, $2 - y$, $1 - z$; iv = $1 + x$, $1 + y$, z; v = $-x$, y, $-z + ^3/_2$; and vi = x, $-y + 1$, $z - ^1/_2$.

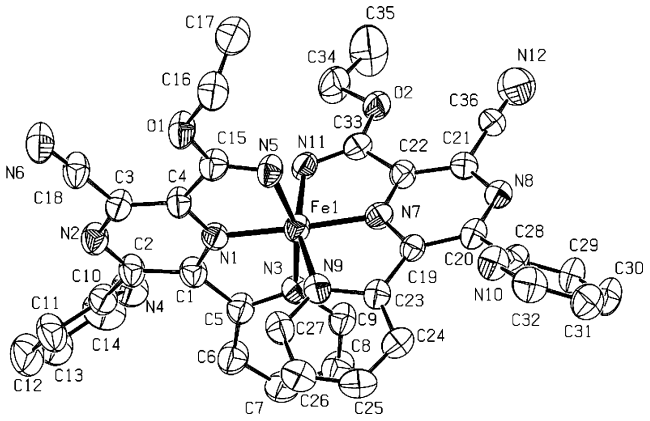

Figure 1. ORTEP diagram of $[Fe(L1')_2]^{2+}$ (**1**) with atomic numbering scheme and thermal ellipsoids at 50% probability level. Hydrogen atoms have been omitted for clarity.

Scheme 1. Ring Numbering Scheme for Complex **1**

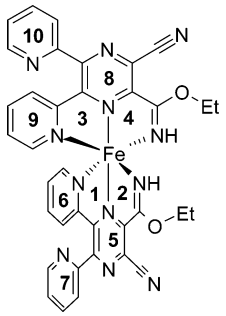

standard values[29] for Fe^{II} compounds in their low-spin (LS) state (1.958, 1.969 Å), and the Fe−N_{pz} bond distances of 1.877(5) and 1.875(5) Å are slightly shorter. These ligands are known to induce a high ligand field strength, and therefore, the metals are expected to be in their LS state. The dihedral angle between the two coordinated pyridine rings is 69.8°. A deviation from planarity of less than 10° can be observed for the unit formed by the rings **3**, **4**, **8**, and **9**, as well as for the unit formed by the rings **1**, **2**, **5**, and **6** (see Scheme 1 and Table 2). The two noncoordinated pyridine rings are quite twisted with respect to these pseudoplanar moieties (42.75° and 50.31°). The four chelate bite angles are similar to those found in other diimine[30] or imido−ester[11−17] complexes. The C═N bond distances of 1.285(8) and 1.293(8) Å are very close to the standard value[29] of 1.279 Å for a C═N double bond distance. Both C15 and C33 possess a rather planar geometry (sp^2 character) as it can be deduced from the values of the angles N═C−C that are very close to 120°. In agreement with the results obtained by Bu et al. from the nickel-mediated methanolysis product,[17] only the *E* imido−ester configuration is observed. In fact, this is the only possibility if a highly stabilized tridentate chelating unit is to be formed and corresponds to the *cis* (outside attack) addition of the alcohol to the nitrile. Steric hindrance reasons disfavor the formation of the *Z* isomer. One nitrile group of each ligand remains unhydrolyzed (see C≡N distances). As already reported by Cini et al.,[11] the 1.325(7) Å mean distance found for C15−O1 and C33−O2 is halfway between those of single and double carbon−oxygen bonds indicating partial double bond character and, therefore, shows the existence of an electron delocalized system over the N−C−O moiety. The 3D packing of complex **1** is influenced by some weak intermolecular N−H···O and C−H···N interactions (see Figure 2). The shortest are found for N11···O16^{i} (i = $^3/_2 - x$, $^1/_2 + y$, $^1/_2 - z$) and C7···N12^{ii} (ii = $-1 + x$, y, z) with distances of 2.965(8) and 3.434(8) Å, respectively.

The IR spectrum of **1** shows the weak ν(C≡N) band at 2243 cm^{-1}, which is unshifted with respect to the free ligand, a very strong band at 1661 cm^{-1} assignable to ν(C═N), and a medium intensity band at 3290 cm^{-1} assignable to ν(N−H). The bands observed at 1270−1199 cm^{-1} can be assigned to the ν(C−O−C) vibrations. Complex **1** is soluble in several solvents such as CH_3CN or MeOH. The positive ES-MS spectrum in CH_3CN exhibits one peak at *m*/*z* 358, assigned to $[Fe(L1')_2]^{2+}$, which corresponds to the solid state compound indicating its stability in solution. On the other hand, when the same experiment is done in MeOH, in addition to the $[Fe(L1')_2]^{2+}$peak, two additional peaks are observed at *m*/*z* 344 and 851 and were assigned to $[Fe(L1\text{-}OMe)_2]^{2+}$ and $[Fe(L1\text{-}OMe)(L1')(CF_3SO_3)]^{+}$, respectively. They correspond to the total and partial methanolysis adducts, respectively. When carried out in a $EtOH/H_2O$ mixture, the ES-MS spectrum still presents the original $[Fe(L1')_2]^{2+}$ peak associated with a water molecule (*m*/*z* 367) and, in addition, a peak at *m*/*z* 303 that corresponds to the protonated form of the monoamido free ligand. Mössbauer spectral measurements at 293 and 135 K were carried out and corroborate the low-spin state of the Fe^{II}. The isomeric shift of 0.138 mm s^{-1} and the quadrupole splitting of 0.45 mm s^{-1} are characteristic for a low-spin Fe^{II} ion in a distorted octahedral environment.

A mechanism for the alcoholysis reaction of L1 to form complex **1** is proposed in Scheme 2. It is reasonable to suppose that, at first, one Fe^{II} ion coordinates to two pyridine and two pyrazine units of two L1 molecules. This will activate the two closest nitrile groups toward the addition of ethanol. In effect, the nitrile carbon atom becomes more electrophilic, and this facilitates the nucleophilic attack of the oxygen electron pair of the alcohol. Once this addition is produced, the imido−ester nitrogen atoms can easily coordinate to the Fe^{II} ion that then achieves its octahedral geometry. Finally, proton transfer from the alcohol oxygen atom to the imido nitrogen atom will lead to the formation of compound **1**. The facility in which this alcoholysis reaction takes place seems to depend on the alcohol used. When methanol is used, the reaction occurs immediately and needs no heating, whereas with propanol, the reaction needs reflux and longer reaction time also due to lower solubility of the reactants. Preliminary studies show that when the reaction is carried out using Co^{II} instead of Fe^{II}, the alcoholysis reaction takes place as shown by the analysis of the ES-MS spectrum (peak at *m*/*z* 359 assigned to $[Co(L1')_2]^{2+}$). On the

(29) *International Tables for Chrystallography C*; Kluwer Academic Publishers: Dordrecht, The Netherlands, 1995.
(30) (a) Grove, H.; Sletten, J.; Julve, M.; Lloret, F.; Lezama, L. *Inorg. Chim. Acta* **2000**, *310*, 217. (b) Chesnut, D. J.; Kusnetzow, A.; Birge, R. R.; Zubieta, J. *Inorg. Chem.* **1999**, *38*, 2663. (c) Figgis, B. N.; Reynolds, P. A.; Lehner, N. *Acta Crystallogr.* **1983**, *B39*, 711. (d) Fijiwara, T.; Iwamoto, E.; Yamamoto, Y. *Inorg. Chem.* **1984**, *23*, 115.

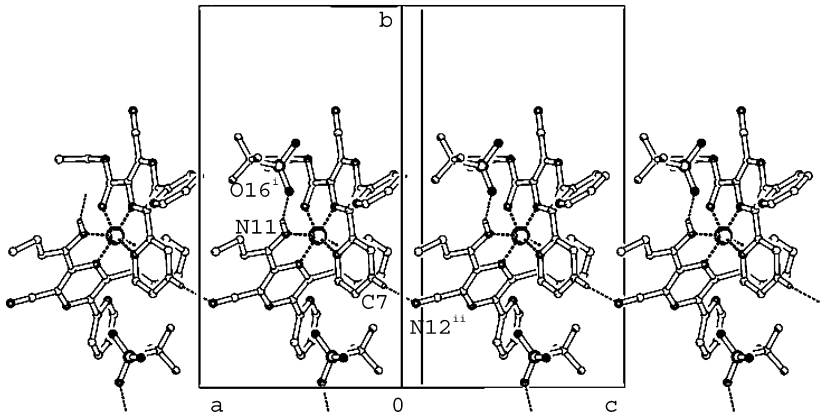

Figure 2. Crystal packing of **1** showing the hydrogen bonding. Only hydrogen atoms involved in hydrogen bonds are shown.

Scheme 2. Proposed Mechanism for the Formation of Complex **1**: Ethanolysis Reaction

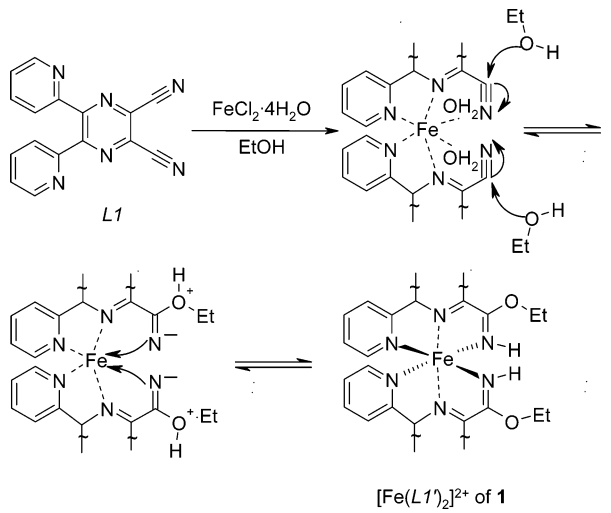

other hand, the reaction with Ag^{I} affords a deep yellow microcrystalline powder. The peaks at *m*/*z* 677 and 391 observed in the ES-MS, assigned to $[Ag(L1)_2]^+$ and $[AgL1]^+$, respectively, indicate that the ligand has not been transformed.

Complex 2. The crystal structure of **2** consists of a mononuclear tripositive Fe^{III} (LS) complex, with three perchlorate units as counterions. Each of the two $(py)_2(pzH\text{-}pyH^+)(O^-)$ moieties act as zwitterion tridentate N,O,N-donor ligands (see Figure 3). The donor atoms surrounding the iron ion are disposed in an octahedral geometry where four pyridyl nitrogen atoms of two different ligand molecules occupy the equatorial plane and the two *trans* oxygen alcoholate atoms occupy the axial positions. The Fe−N and Fe−O bond lengths (Table 2) agree with the expected values for $Fe-N_{py}$ (1.969 Å) and $Fe-O_{alkoxy}$ (1.817 Å) in comparison with the standard values.[29] The O1−Fe1−O2 axis is close to linearity and so are the N4−Fe1−N25 and N5−Fe1−N24 axes. The main structural features of the mononuclear Re complex reported by Bandoli et al.[20] and complex **2** are comparable (see Scheme 3, Table 2). The major difference is that the twisting between the coordinated pyridine rings is greater in complex **2** (86.52° and 83.53°) than in the Re complex (69.2°). This effect may come from the shorter Fe−N or Fe−O distances compared to Re−N

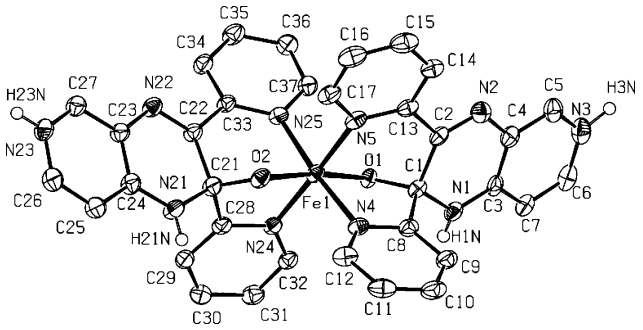

Figure 3. ORTEP diagram of *R*,*R*-$[Fe(L2')_2]^{3+}$ (**2**) with atomic numbering scheme and thermal ellipsoids at 50% probability level. Only four relevant H atoms are shown; the rest have been omitted for clarity.

Scheme 3. Ring Numbering Scheme for Complex **2**

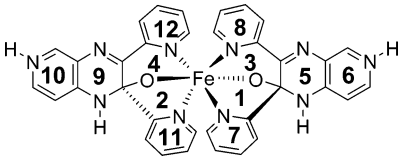

and Re−O. Compound **2** contains two chiral centers, C1 and C21, and as the space group is centrosymmetric, the overall structure is the racemic mixture of the two *R*,*R* and *S*,*S* enantiomers. Atoms C2 and C22 possess sp^2 character, and the distances C2−N2 and C22−N22 are in good agreement with the standard value of 1.279 Å for a C=N double bond distance. Interatomic contacts in the crystal packing have been observed between the complex molecules and the perchlorate anions and solvent molecules. Table 2 contains a list of the most relevant N−H···O and N−H···N hydrogen bonds present in this compound.

The IR spectrum of **2** exhibits a number of strong peaks in the region from 1646 to 1471 cm^{-1} assigned to ν(arC−N) and ν(arC−C) vibrations and a medium intensity band at 3245 cm^{-1} assignable to ν(N−H). The stretching mode ν(+−NH=) may be tentatively assigned to the 2256 cm^{-1} peak. The band at 1238 cm^{-1} can probably be assigned to the ν(C−O) vibrations. The noncoordinated ClO_4^- anions show the expected vibration at 1159−1102−1044 cm^{-1}. The ES-MS spectrum in acetonitrile supports the stability of **2** in solution with the peaks at *m*/*z* 660 and 330 assigned to $[Fe(L2')_2 - 2H^+]^+$and $[Fe(L2')_2 - H^+]^{2+}$, respectively. In order to establish the spin state of the Fe^{III} center in complex

Scheme 4. Proposed Mechanism for the Formation of Complex **2**: Hydration Reaction

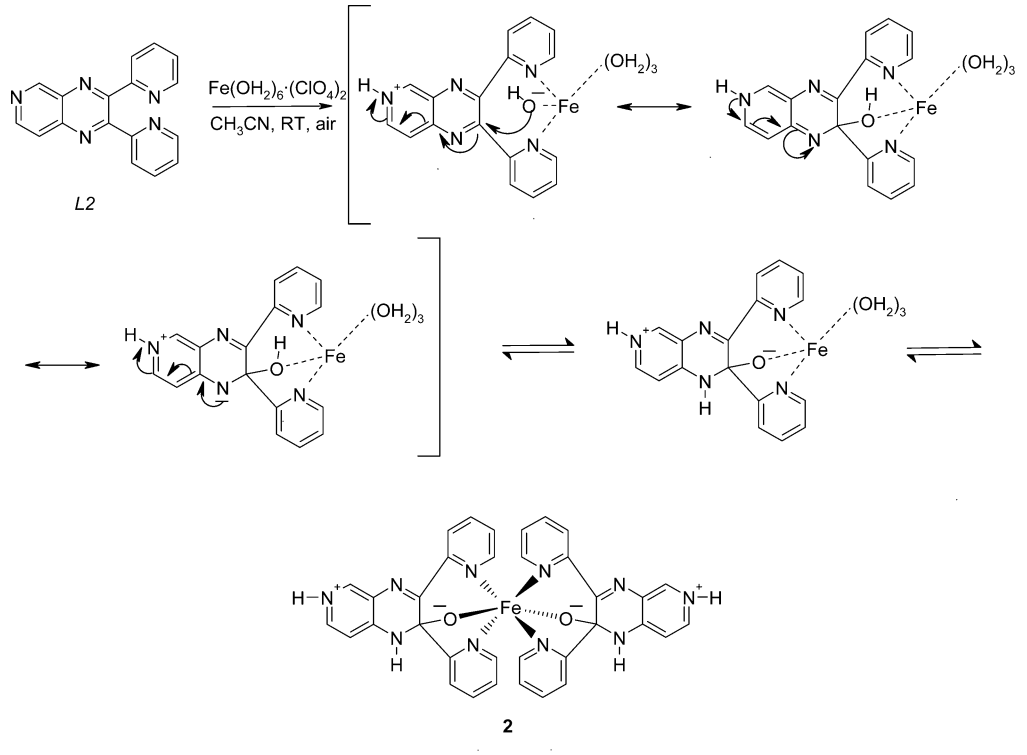

2, variable temperature magnetic susceptibility measurements were performed. The $\chi_M T$ value of 0.36 emu·K/mol at 300 K corresponds to an $S = {}^1/_2$ state and, thus, to the low-spin state.

As for compound **1**, a mechanism of the nucleophilic addition of water to L2 is proposed in Scheme 4. In this reaction, the hydrated Fe^{II} acts as a Lewis acid being able to activate its coordinated water molecules and making easier the protonation of the ligand nitrogen atoms. The protonation of the pyridine nitrogens N3/N23 is favored by the formation of a stabilizing resonant intermediate. At the same time, the metal center coordinates to the pyridine rings of one or two ligand molecules. At this stage, two hydroxyl groups will be in good positions to attack the imino carbons C1 and C21. In this manner, the Fe^{II} ion can complete its octahedral coordination geometry, and the seven-membered ring strain is reduced (change from sp^2 to sp^3 at C). The last reaction steps may be the proton transfer from the hydroxyl group to the pyrazine nitrogen and the air-oxidation of Fe^{II} to Fe^{III} to afford compound **2**. The reaction can take place between one Fe center and one ligand molecule and then, in a further step, with a second ligand molecule or simultaneously between one Fe ion and two ligand molecules.

Complex 3. The structure of *trans*-[FeL2″Cl_2] (**3**) contains neutral mononuclear Fe^{III} (HS) complexes (Figure 4) with the metal ion located on a 2-fold axis. The Fe^{III} center is bounded in the equatorial plane to a tetradentate deprotonated bis(carboxamido) unit and axially to two chlorine atoms so adopting a strongly distorted octahedral geometry (see Table 2 and Scheme 5). The Fe−N_{amide}, Fe−$N_{pyridine}$, and Fe−Cl bond distances are almost identical to those reported for the high-spin Fe^{III} complex [Et_3NH][Fe(bpb)Cl_2]·CH_3CN (H_2bpb = 1,2-bis(2-pyridinecarboxamido)benzene).[31] In the low-spin

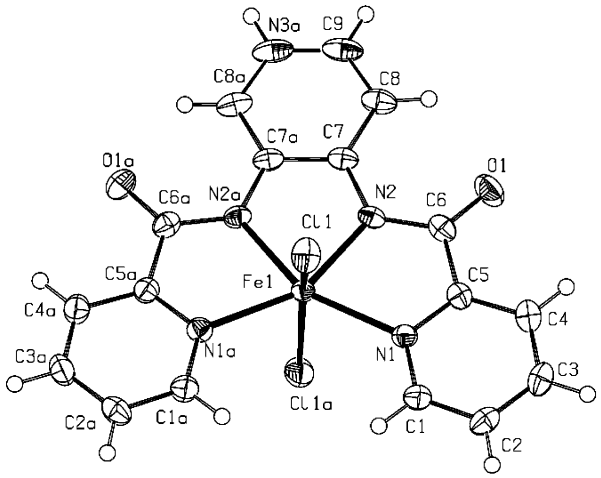

Figure 4. ORTEP diagram of complex *trans*-[FeL2″Cl_2] (**3**) with atomic numbering scheme and thermal ellipsoids at 50% probability level.

Scheme 5. Ring Numbering Scheme forComplex **3**

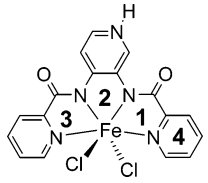

complex [Fe(bpb)(1-MeIm)$_2$](ClO$_4$),[32] the Fe−N_{amide} and Fe−$N_{pyridine}$ distances are notably shorter. The C−O, C_{py}−N, and $C_{carboxy}$−N distances do not vary with a change in the spin state of the metal ion. These and other Fe^{III}

(31) Yang, Y.; Dietrich, F.; Valentine, J. S. *J. Am. Chem. Soc.* **1991**, *113*, 7195.
(32) Che, C.-M.; Leung, W.-H.; Li, C.-K.; Cheng, H.-Y.; Peng, S.-M. *Inorg. Chim. Acta* **1992**, *196*, 43.

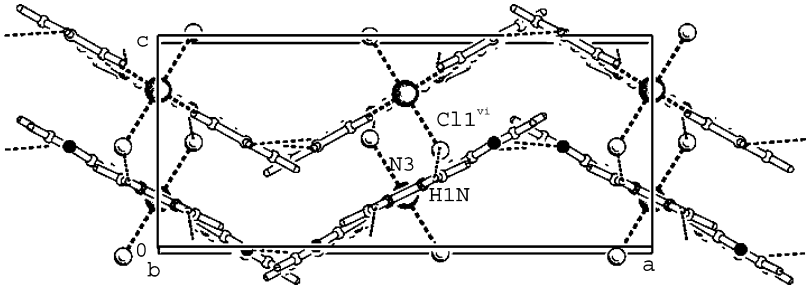

Figure 5. Crystal packing of **3** down the *b* axis with the hydrogen-bonding pattern.

Scheme 6. Proposed Mechanism for the Formation of Complex **3**: Hydration−Oxidation Reaction

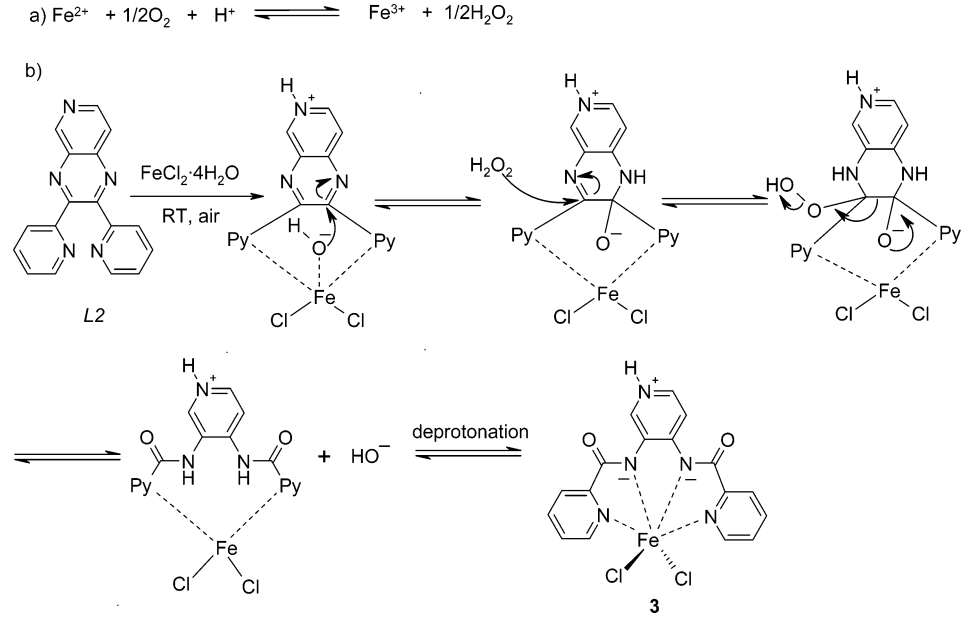

mononuclear complexes of a series of ligands related to H_2bpb have been reported.[33,34] It has been observed that it is possible to tune the spin state of the Fe^{III} center by varying the axial substituents. For complex **2**, variable temperature magnetic susceptibility measurements were performed to establish the spin state of the Fe^{III} center. The $\chi_M T$ value of 4.54 emu·K/mol corresponds, as expected for chlorine axial ligands, to an $S = {}^5/_2$ state and, thus, to the high-spin state. This value remained constant over the temperature range (300−1.8 K) of the measurement. It is interesting to note that, in related low-spin complexes, the axial ligands are almost linearly arranged whereas in the high-spin ones, the angle X−Fe−X is always about 150° (in our case, 155.40(5)°).[34] Concerning the crystal packing, the shortest interaction between symmetry related molecules is found for N3···Cl1^a, a = x, $-y$ 1, $z - {}^1/_2$, with a distance of 3.346(3) Å (Figure 5 and Table 2). Due to these contacts, the molecules are disposed, down the *b* axis, in a manner that confers a zigzag shape to the packing.

The IR spectrum of **3** confirms that the ligand is deprotonated; no amide ν(N−H) band is observed. The amide ν(C═O) and ν(C−N) bands appear in the region 1654−1570 cm^{-1}. Complex **3** is rather insoluble and forms a dark suspension in alcohols or acetonitrile, but it is soluble in water giving an orange clear solution. We have observed that complex **3** dissolves in DMF after heating for some time to give a red-pink solution. The ES-MS spectrum in MeOH presents two peaks at *m*/*z* 409 and 320 assignable to $[FeL2''Cl]^+$ and $[H_2L2'']^+$, respectively, while in H_2O two peaks at *m*/*z* 409 and 374 can be assigned to $[FeL2''Cl]^+$and $[FeL2'']^{2+}$ species. This suggests that, in solution, the axial ligands can be dissociated or displaced from the complex, but the bis(carboxamido) unit complex is stable.

The formation of this complex appears to involve several reaction steps. We have observed, as already indicated in the Experimental Section, that when the reaction was carried out under anaerobic conditions in a sealed H-tube, a few crystals of **3** started to appear only after several months. On the other hand, when the reaction was done with stirring under aerobic conditions, complex **3** precipitated from the solution after a short time and in good yield. These signs imply that the reaction requires the presence of oxygen. It is rather complicated to propose a suitable mechanism. Nevertheless, a proposal is given in Scheme 6. It seems reasonable to suppose that an intermediate of the type of complex **2** could be formed in a first stage (including protonation of the pyridine ring, coordination of the metal,

(33) (a) Patra, A. K.; Ray, M.; Mukherjee, R. *Inorg. Chem.* **2000**, *39*, 652. (b) Patra, A. K.; Mukherjee, R. *Polyhedron* **1999**, *18*, 1317. (c) Ray, M.; Mukherjee, R.; Richardson, J. F.; Buchanan, R. M. *J. Chem. Soc., Dalton Trans.* **1993**, 2451.

(34) Dutta, S. K.; Beckmann, U.; Bill, E.; Weyhermüller, T.; Wieghardt, K. *Inorg. Chem.* **2000**, *39*, 3355.

and nucleophilic attack of one water molecule), the main difference being the presence now of two terminal chlorine atoms. The Fe^{II} can be air oxidized to Fe^{III} (subreaction a in Scheme 6) with the consequent formation of hydrogen peroxide.[35] This oxidation can either precede or follow the addition of water to the ligand. The peroxide anions might then attack the hydrated molecule leading to the oxidative cleavage[24] of the pyrazine C−C bond generating, as a result, a diamide moiety and, after a final deprotonation step, complex **3**, as it appears in the crystal structure.

In conclusion and to sum up, three interesting examples have been presented where a metal ion, in this case, iron, serves as a Lewis acid and induces polarization through the ligand. In the alcoholysis of nitriles, the attack of the alkoxy O atom is the rate-limiting step, and the iron center is able to accelerate it. This catalytic effect is associated with a gain in stability based on the formation of coordinative bonds. On the other hand, the expected coordination mode of L2 to metal ions is via its bipyridine-type units to form a stable five-membered ring. In our case, it seems instead that the Fe^{II} ion coordinates to the pyridine rings of one or two ligand molecules to form a strained seven-membered ring. The nucleophilic attack of water serves in this case to reduce the steric strain. The results reported in this study contribute to the field of reactions of coordinated ligands and could be helpful in the understanding of the very important role of the metal ions in a large variety of chemical processes. The mechanisms proposed for the formation of these three complexes are hypothetical. More detailed studies would be necessary to affirm how these transformations take place and whether any of them could be used, for instance, in catalysis. It would also be interesting to explore the use of complex **3** as a building block for materials with new magnetic properties profiting from the fact that the two chloride axial ligands may be displaced by other ligands such as CN^-, SCN^-, and N_3^-, leading to the formation of polymeric chains or other types of arrangements. As a preliminary result, we have already obtained the crystal structure of the analogue of complex **3** with CN^- as axial ligands. Further investigations will continue in this direction.

(35) Hughes, M. N. *The Inorganic Chemistry of Biological Processes*, 2nd ed.; John Wiley & Sons Ltd.: New York, 1981; Chapter 7.

Acknowledgment. Support for this research by the Swiss National Science Foundation, Grant 20-61641.00, is gratefully acknowledged.

Supporting Information Available: Crystallographic files for **1**−**3** in CIF format. This material is available free of charge via the Internet at http://pubs.acs.org.

IC026079L